

# Broadband Focusing with Double-gradient Multilayers

C. Morawe,<sup>1</sup> J.-C. Peffen,<sup>1</sup> E.M. Dufresne,<sup>2</sup> Y.S. Chu,<sup>3</sup> A.T. Macrander<sup>3</sup>

<sup>1</sup>European Synchrotron Radiation Facility (ESRF), Grenoble, France

<sup>2</sup>Department of Physics, University of Michigan, Ann Arbor MI, U.S.A.

<sup>3</sup>Advanced Photon Source (APS), Argonne National Laboratory, Argonne, IL, U.S.A.

## Introduction

Periodic multilayers used in third-generation synchrotron optics reflect x-rays in a bandwidth of a few percent. They are therefore a convenient alternative for bridging the gap between perfect crystals and total reflection mirrors. To further increase the effective bandwidth, nonperiodic or depth-graded layered structures can be designed [1, 2]. Focusing or collimating multilayer optics generally require a lateral thickness gradient to account for the variation of the incident angle [3, 4] given by the geometry. It would be desirable to merge the lateral and depth gradient techniques into one device. This would allow for the design of a focusing mirror with a fixed focal distance and large beam acceptance over a reasonably wide energy range.

The concept is illustrated in Fig. 1 and is similar to that of DuMond diagrams [5]. In the energy dispersion relationship  $E = E(\theta)$  (Bragg equation), the angular dependence has to be interpreted in terms of the distance  $f$  from the position on the mirror to the focal point — that is,  $\theta = \theta(f)$  — leading to  $E = E(f)$ .

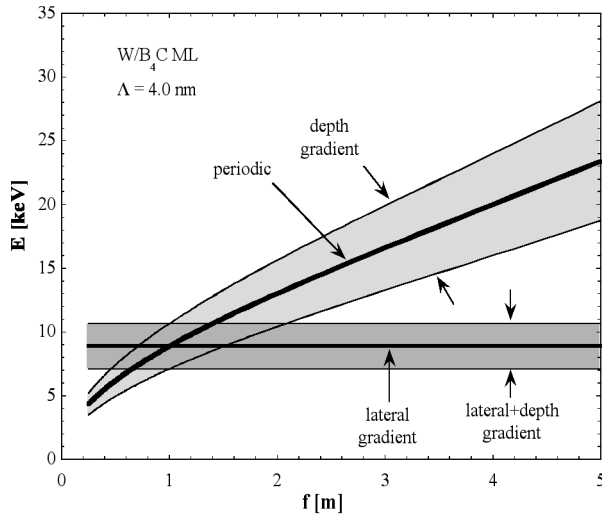


FIG. 1. Energy dispersion of different types of multilayers. Thick solid lines represent periodic multilayers, either with or without a lateral thickness gradient. A purely depth-graded, nonperiodic multilayer covers the zone in lighter gray. A combination of lateral and depth gradient is indicated by the area in darker gray.

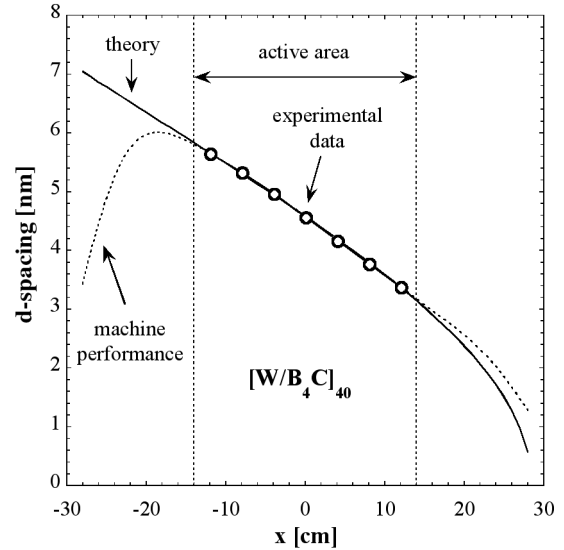


FIG. 2.  $W/B_4C$  multilayer  $d$ -spacing along the length of the mirror. The solid line is the ideal curve obtained from geometrical considerations. The broken line takes into account the performance of the coating facility. Open circles show experimental data points derived from x-ray reflectivity scans.

## Methods and Materials

We followed the ideas outlined above to design and fabricate a double-graded, focusing, multilayer mirror on the basis of a simple bending device and a preshaped substrate [6]. The mirror shape is parabolic, with a length of 270 mm, a focal distance  $f$  of 285 mm, and an angle of incidence  $q$  of  $0.93^\circ$  at the mirror center. The design of the lateral  $d$ -spacing variation was done for a mean energy of 9 keV.  $W$  and  $B_4C$  were chosen as coating materials because of the strong optical contrast in this energy range.

Figure 2 shows the  $d$ -spacing of the multilayer along the total active length of the mirror, indicating the steep lateral gradient necessary to reflect the x-rays at every point of the mirror.

The additional thickness variation with depth was added by using the center of the mirror as a reference point. The goal was to enlarge the intrinsic bandwidth of a periodic  $W/B_4C$  multilayer (4-5%) to about 9% and to provide a flat plateau with a constant reflectivity of 50%. The circles in Fig. 3 show the layer sequence after

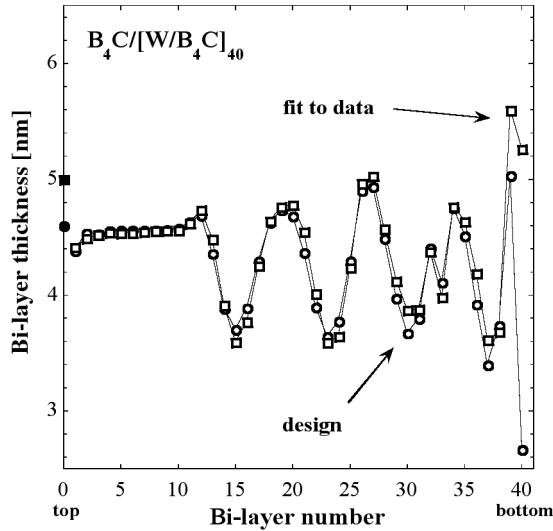


FIG. 3. Experimental bi-layer thickness versus bi-layer number at the center of the  $W/B_4C$  multilayer (squares) after numerical refinement compared to the design goal (circles). Protecting  $B_4C$  layers are indicated separately (solid symbols). The lines are guides to the eye.

the optimization procedure. Forty periods were chosen to obtain the required performance. A purely numerical refinement routine based on a least-square-fit algorithm was applied.

The multilayer was characterized by  $\theta:2\theta$  x-ray reflectivity scans taken on a fixed anode reflectometer at  $E = 8048$  eV, followed by numerical simulation of the data. The open circles in Fig. 2 indicate the experimental lateral thickness gradient and confirm the good agreement with theory. In Fig. 3, the addition of experimental bi-layer thickness taken from fits to the reflectivity data is shown by squares.

Focusing experiments were carried out at MHATT-CAT undulator beamline 7-ID at the APS. In order to image the focused beam, a lens-coupled charge-coupled device (CCD) with  $1000 \times 1000$  pixels was used. In it, the visible light that was produced by the x-rays striking the scintillator was magnified by an objective lens and detected by the CCD. The effective pixel resolution for the experiment using  $5\times$  objective magnification was  $1.34 \mu\text{m}$ . The point spread function of the scintillator was determined to be about  $2 \mu\text{m}$ . The CCD system was mounted 285 mm from the center of the multilayer. An ion chamber was placed 157 cm upstream from the multilayer to monitor the primary intensity. The beam was reflected and focused horizontally. The curvature of the multilayer was pre-set on the optical long-trace profiler (LTP) of the APS metrology laboratory and then refined *in situ* by using x-rays and the CCD camera. Several series of scans were taken with fixed

focusing geometry while the photon energy of the incoming beam was varied. This was done by simultaneously moving the undulator gap and directing the x-rays into the fixed-exit double-Si-crystal monochromator [7].

## Results

The multilayer was exposed at 9.1 keV with a beam of 1.5 mm in the horizontal direction and 1.0 mm in the vertical direction. Figure 4 shows a cross section through the focal line. From a Gaussian fit to the data, one extracts a full width at half maximum (FWHM) of about  $S_{\text{EXP}} = 8 \mu\text{m}$ . With a source distance of 54 m and a focal distance of 285 mm, one obtains a geometrical demagnification of 0.00528. Since the horizontal source size (FWHM) is about  $830 \mu\text{m}$ , one would expect a source-limited line width of  $S_S = 4.4 \mu\text{m}$ . The measured figure error of the flat mirror contributes about  $S_{\text{FE}} = 4.0 \mu\text{m}$  to the total line width. By adding the squares of all relevant sources of line broadening, one obtains a theoretical estimate of  $S_{\text{TH}} = 6.3 \mu\text{m}$ , which represents a lower limit compared to the measured  $8 \mu\text{m}$ .

Figure 5 shows the measured total intensity (circles) of the focal line plotted versus the photon energy, compared with the ideal spectrum as obtained from theoretical simulations (dashed line). The shape difference is mainly due to the attenuation caused by absorbing Al windows and by the air path between the ion chamber and the CCD. The energy shift of  $-220$  eV is within the error margin of the alignment and focusing procedure. The solid line indicates a simulation that

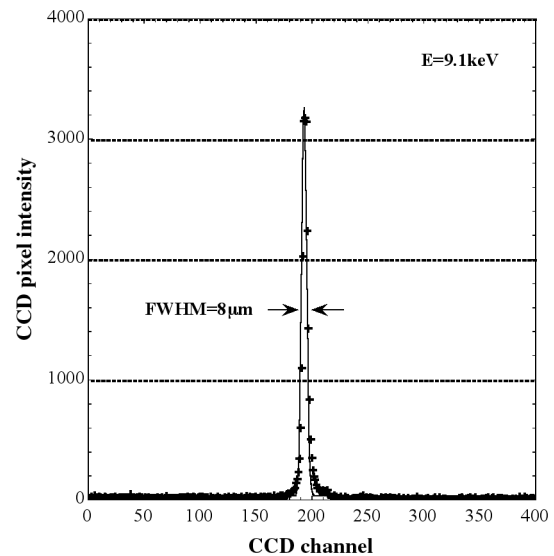


FIG. 4. Cross section through the focal line. To improve the signal-to-noise ratio, the intensity was averaged over 5 central pixel rows. The experimental data (+) were fitted by a Gaussian function.

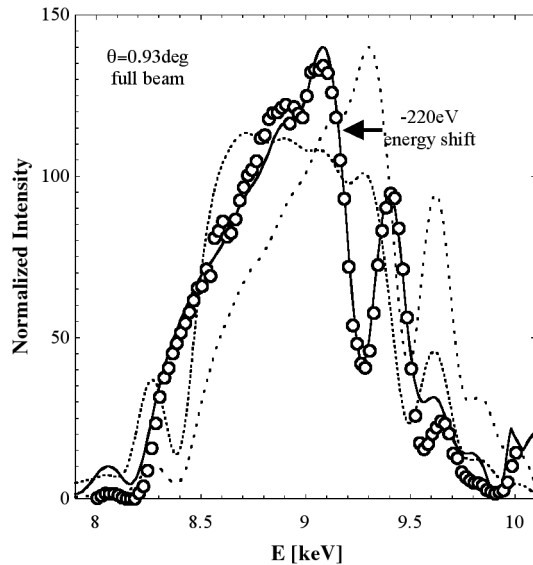


FIG. 5. Normalized total intensity of the focal line measured on the CCD detector (circles) versus photon energy. The background was removed. The dashed line indicates the ideal spectrum, the dotted line includes absorption corrections, and the solid line contains an additional energy shift.

accounts for the above effects. In this case, all main features of the measured data can be reproduced.

The position of the focal line during the above energy scan was stable within a margin of 5  $\mu\text{m}$ , and the FWHM of the focus remained stable between 7 and 8  $\mu\text{m}$ .

## Discussion

It has been shown that combining the lateral and vertical thickness variations in multilayered structures is feasible from a theoretical as well as from a practical point of view. On the basis of a simple setup, a multilayer focusing device was designed, fabricated, and tested. It provides a fixed focusing geometry while offering a broad and flat energy response of about 10%. It therefore combines the advantage of the wide energy range of a total reflection mirror with the increased angle of incidence of a multilayer.

The focusing experiments have shown that the double-graded multilayer performs approximately as expected. Special care has to be taken with regard to the experimental conditions, particularly during sample

alignment and monitoring of the total intensity. The size of the focal line is clearly limited by the moderate substrate quality and by the relatively simple bending device. An improvement of the focal spot would be straightforward by using a state-of-the-art dynamical bender [8] equipped with a low-figure-error substrate.

In the present case, the high absorption, the steep lateral gradient, and the strong geometrical effect on the local flux density provoke a huge intensity variation along the curved multilayer. This means that designing the depth gradient is a challenging task. Most applications on third-generation synchrotron beamlines, however, require less severe boundary conditions than those discussed above. Photon energies above 10 keV and less pronounced lateral gradients significantly facilitate design and fabrication. Further efforts will be made to integrate such devices into ESRF beamline optics.

## Acknowledgments

The authors would like to thank A. Rommeveaux from the ESRF optics group and L. Assoufid from the APS optics group for their cooperation on the metrology measurements, as well as D. Arms from MHATT-CAT and P. Ilinsky from the APS x-ray microscopy group for their experimental assistance. Use of the APS was supported by the U.S. Department of Energy, Office of Science, Office of Basic Energy Sciences, under Contract No. W-31-109-ENG-38.

## References

- [1] V.V. Protopopov, Proc. SPIE **4144**, 116 (2000).
- [2] C. Morawe, E. Ziegler, J.-C. Peffen, and I.V. Kozhevnikov, Nucl. Instrum. Methods A **493**, 189 (2002).
- [3] M. Schuster, H. Göbel, L. Brügemann, D. Bahr, F. Burgäzy, C. Michaelsen, M. Störmer, P. Ricardo, R. Dietsch, T. Holz, and H. Mai, Proc. SPIE **3767**, 183 (1999).
- [4] C. Morawe, P. Pecci, J.-C. Peffen, and E. Ziegler, Rev. Sci. Instrum. **70**, 3227 (1999).
- [4] J.W.M. DuMond, Phys. Rev. **52**, 872 (1937).
- [5] C. Morawe, J.-C. Peffen, E.M. Dufresne, Y.S. Chu, and A.T. Macrander, Proc. SPIE **5195** (2003).
- [6] E.M. Dufresne, D.A. Arms, S.B. Dierker, R. Clarke, Y. Yacoby, J. Pitney, B. MacHarrie, and R. Pindak, Rev. Sci. Instrum. **73**, 1511 (2002).
- [7] O. Hignette, P. Cloetens, W.-K. Lee, W. Ludwig, and G. Rostaing, J. Phys. IV **104**, 231 (2003).